Quantification of *Feline immunodeficiency virus* (FIV_{pco}) in peripheral blood mononuclear cells, lymph nodes and plasma of naturally infected cougars

David J. Blake,[1] Jon Graham[2] and Mary Poss[1]

Division of Biological Sciences[1] and Department of Mathematical Sciences[2], University of Montana, HS104, Missoula, MT 59812, USA

Correspondence
Mary Poss
mary.poss@umontana.edu

Received 22 August 2005
Accepted 20 December 2005

Infection of domestic cats with *Feline immunodeficiency virus* (FIV) results in a fatal immunodeficiency disease, similar to *Human immunodeficiency virus 1* (HIV-1) in humans. Elevated plasma viral loads in domestic cats are correlated to decreased survival time and disease progression. However, FIV is also maintained as an apathogenic infection in other members of the family Felidae including cougars, *Puma concolor* (FIV_{pco}). It is not known whether the lack of disease in cougars is a result of diminished virus replication. A real-time PCR assay was developed to quantify both FIV_{pco} proviral and plasma viral loads in naturally infected cougars. Proviral loads quantified from peripheral blood mononuclear cells (PBMC) ranged from $2{\cdot}90 \times 10^1$ to $6{\cdot}72 \times 10^4$ copies per 10^6 cells. Plasma viral loads ranged from $2{\cdot}30 \times 10^3$ to $2{\cdot}81 \times 10^6$ RNA copies ml^{-1}. These data indicate that FIV_{pco} viral loads are comparable to viral loads observed in endemic and epidemic lentivirus infections. Thus, the lack of disease in cougars is not due to low levels of virus replication. Moreover, significant differences observed among cougar PBMC proviral loads correlated to viral lineage and cougar age ($P = 0{\cdot}014$), which suggests that separate life strategies exist within FIV_{pco} lineages. This is the first study to demonstrate that an interaction of lentivirus lineage and host age significantly effect proviral loads.

INTRODUCTION

Feline immunodeficiency virus (FIV) is a lentivirus that infects members of the family Felidae worldwide. Although all FIV strains detected in wild and domestic cats form a monophyletic cluster in a phylogeny of lentiviruses, each feline species is infected with a distinct virus and infection results in disparate outcomes (Burkhard & Dean, 2003). FIV is maintained as an apathogenic infection in some members of the cat family such as lions (*Panthera leo*) and cougars (*Puma concolor*) (Biek *et al.*, 2005; Brown *et al.*, 1994; Carpenter & O'Brien, 1995; Olmsted *et al.*, 1992; Packer *et al.*, 1999). However, FIV infection in domestic cats results in a disease similar to that caused by *Human immunodeficiency virus 1* (HIV-1) infection in humans that begins with an acute illness and progresses to immunodeficiency and ultimately death (Pedersen *et al.*, 1987).

The amount of circulating virus is a strong prognostic indicator for disease progression in FIV and HIV-1 infections (Goto *et al.*, 2002; Mellors *et al.*, 1996). In both naturally and experimentally infected domestic cats, FIV replicates to high titres and elevated viral loads are associated with shorter survival time and progression to feline acquired immunodeficiency syndrome (AIDS) (Diehl *et al.*, 1996; Goto *et al.*, 2002). Similarly, high plasma virus loads are associated with disease progression in HIV-1 (Mellors *et al.*, 1996).

African primates are also host to lentivirus infections (simian immunodeficiency virus, SIV) and, as is the case with endemic feline lentivirus infections, there is no evidence of disease (Beer *et al.*, 1996; Broussard *et al.*, 2001). However, plasma virus loads in African green monkeys (*Cercopithecus aethrops*) and sooty mangabeys (*Cercocebus ayts*) naturally infected with SIV_{agm} and SIV_{sm}, respectively, are in the order of 10^6 RNA copies ml^{-1} (Broussard *et al.*, 2001; Chakrabarti, 2004). These data indicate that virus replication can be robust even in asymptomatic infections and thus high levels of circulating virus are not always associated with disease.

The GenBank/EMBL/DDBJ accession numbers for the sequences reported in this paper are AY120787, AY120790, AY120793–AY120794, AY120798–AY120802, AY120804–AY120810, AY120812, AY120815, DQ106994–DQ106997, DQ106999–DQ107000, DQ107003–DQ107006, DQ107052–DQ107054, DQ107056–DQ107060 and DQ107062–DQ107068.

Currently, no viral load data have been determined for endemic FIV infections in wild felids. FIV_{pco} infects free-ranging cougars in North and South America with infection prevalence averaging 30 % (Carpenter *et al.*, 1996), but reaching as high as 58 % in some populations in western USA (Biek *et al.*, 2003). This prevalence is remarkable because cougars are solitary carnivores with infrequent conspecific contacts. Intrahost viral diversity is less than 1 % in infected cougars and the evolutionary rate of FIV_{pco} has been estimated at 0·1–0·3 % per site per year (Biek *et al.*, 2003). This is an order of magnitude lower than the estimated rate of 3 % per site per year reported for SIV_{agm} (Muller-Trutwin *et al.*, 1996) or 1 % per site per year for HIV-1 (Shankarappa *et al.*, 1999). The faster evolutionary rate of SIV and HIV-1 could be due to increased virus replication resulting in a rapid accumulation of mutations and stronger selection on the virus population. Therefore, based on the lack of disease, the low intrahost viral diversity and low evolutionary rates, we hypothesized that FIV_{pco} viral loads in infected cougars would be lower than in pathogenic FIV and HIV-1 infections or in endemic SIV infection in primates. We subsequently developed a real-time PCR assay for FIV_{pco} and used the assay to determine the amount of cell-associated (proviral DNA) and cell-free (viral RNA) virus present in a large set of naturally infected cougars.

METHODS

Study population and cougar samples. Peripheral blood mononuclear cells (PBMC), lymph nodes (LN) and plasma samples used in this study were obtained from free-ranging cougars from four Rocky Mountain populations determined previously to be infected with FIV_{pco}. Genomic DNA samples from PBMC were obtained from 39 infected cougars. Genomic DNA samples from LN were obtained from a group of 10 hunter-killed animals submitted to the Montana Department of Fish, Wildlife and Parks. Plasma samples were also obtained from 32 infected cougars. Genomic DNA was extracted from samples as described previously (Biek *et al.*, 2003).

Phylogenetic analysis. A 779 bp fragment of proviral *env* was amplified from serial dilutions of PBMC or LN DNA from all infected cougars evaluated in this study in order to determine lineage affiliation. PCR products were cloned and sequenced as described previously (Biek *et al.*, 2003). Alignments were conducted in Lasergene (version 5.5) from DNASTAR using the CLUSTAL W algorithm. A maximum-likelihood (ML) tree was created in PAUP* (4.10b; Swofford, 2002) using a GTR + I + G model as determined in MODELTEST (Posada & Crandall, 1998). PLV1695 (AY307116) was used as an outgroup (Biek *et al.*, 2003). One hundred bootstrap iterations were performed. One *env* sequence for each cougar has been submitted to GenBank.

Sequence analysis of real-time FIV_{pco} amplicon. A 690 bp fragment near the 3′ end of *env* was amplified by nested PCR from DNA derived from PBMC of 14 infected cougars, which included representatives of each viral lineage to determine the sequence variation in the FIV_{pco} amplicon primer sites. The oligonucleotides used for the first round were Co7990F (5′-ATGCAAGTTATGAGATGTAG-3′) and Co8958R (5′-TTATTCAACCGTTCGCACTT-3′). The oligonucleotides used for the second round were Co3LTRF (5′-ACGGCCTTAGTGGTGTCTCAG-3′) and Co8859R (5′-CCATTCCTCCCAGTCTACCC-3′). The conditions for the first round of PCR were as follows: 3 min at 94 °C followed by 35 cycles of 94 °C for 30 s, 48 °C for 30 s, 71 °C for 70 s and followed by 5 min extension at 71 °C. The conditions for the second round of PCR were as follows: 3 min at 94 °C followed by 35 cycles of 94 °C for 30 s, 51 °C for 30 s, 71 °C for 45 s and followed by 5 min extension at 71 °C. PCR products were cloned into the pDrive plasmid (Qiagen) and sequenced. The viral sequence from lineage four was an exact match to both the forward and reverse primers. The sequences from lineage one and three had the same single mismatch in the reverse primer. Sequences from lineage two had a single mismatch in the forward primer and those from lineage five had single mismatches in both the forward and reverse primers.

Plasma viral RNA preparation. The total volume of plasma or serum available from each cougar, which ranged from 100 µl to 6·5 ml per infected cougar, was centrifuged for 1·5 h at 100 000 ***g***. The viral pellet was resuspended in 140 µl PBS containing Ca^{2+} and Mg^{2+} and incubated for 1 h with DNase. RNA was purified using the QIAamp viral RNA mini kit (Qiagen) and eluted in 30 µl DEPC-treated water. Where plasma volumes were greater than 2 ml, RNA was eluted in 60 µl DEPC-treated water. Samples were stored at −80 °C until used for cDNA synthesis.

Preparation of DNA and RNA real-time PCR standards. A plasmid standard for myosin was constructed by amplifying a 220 bp fragment of cougar genomic DNA with primers designed to exon 19 of the cougar myosin gene. The primers used were MyoF (5′-CAAGAACTGGCCCTGGATGAA-3′) and MyoR (5′-CTGCACTTGGAGCTGGAGGTC-3′). The conditions for PCR were as follows: 3 min at 94 °C followed by 30 cycles of 94 °C for 30 s, 52 °C for 30 s, 71 °C for 50 s and followed by 5 min extension at 71 °C. PCR product was cloned into the pCR4-Topo plasmid (Invitrogen). For each FIV_{pco} DNA standard, a 690 bp fragment of the FIV_{pco} genome near the 3′ end of *env* was amplified by PCR from cougar proviral DNA as described above. All plasmids were linearized and purified with the QIAquick PCR Purification kit (Qiagen). Plasmid concentration was determined by UV spectroscopy. All DNA plasmid standards were diluted in 10 mM Tris (pH 8·5) containing salmon sperm DNA (Sigma-Aldrich) as a carrier at a final concentration of 6 ng μl^{-1}.

Virus from the supernatant of a co-culture of 3201 cells and PBMC of a naturally infected cougar, SRF631, was used for the RNA standards. Viral RNA concentration was determined by UV spectroscopy to estimate copy number. All RNA standards were diluted in DEPC-treated water with carrier tRNA (Sigma) at a final concentration of 63 ng μl^{-1}. The viral RNA standards and viral RNA obtained from the plasma of infected cougars contained equivalent carrier tRNA concentrations.

FIV_{pco} real-time PCR quantification. TaqMan chemistry was used to quantify the number of cell equivalents in each proviral reaction. For the myosin reactions, the primers used were MyoTaqMF (5′-TGGCCCTGGATGAAACTCTACT-3′) and MyoTaqMR (5′-GCCATCTCCTTCTCGGTCTCT-3′). The probe sequence used for this primer set was Myoprobe (5′-FAM-CAAGATCAAGCCCCTCCTCAAGAGCG-TAMRA-3′).

SYBR green chemistry was used for quantification of FIV_{pco} from genomic DNA and plasma because sequence divergence among FIV_{pco} lineages precluded designing a suitable probe. The primers used were ETaqF (5′-TGATCCTGATGCTCCACCAAC-3′) and ETaqR (5′-TCTCACTCTGTTCTGCCCATT-3′). The amplification with this pair of oligonucleotides produced a fragment of 170 bp.

Reactions consisted of 25 µl 2× Universal Master Mix (Applied Biosystems) containing 100 mM KCl, 40 mM HCl/Tris, 1·6 mM dNTP, 50 U *Taq* μl^{-1}, 6 mM $MgCl_2$ and 5 µl genomic template, in a

50 µl total reaction volume. Each reaction for myosin amplification contained 300 nM MyoTaqMF, 100 nM MyoTaqMR and 50 nM Myoprobe. Each FIV_{pco} proviral reaction contained 300 nM ETaqF, 300 nM ETaqR and 1 : 10 000 dilution of SYBR Green I gel stain (BioWhitaker).

Myosin amplification was as follows: 95 °C for 10 min followed by a two-step PCR procedure consisting of 95 °C for 15 s then 60 °C for 1 min for 45 cycles. FIV_{pco} amplification was similar except that the annealing temperature was at 61 °C for 1 min. Amplification, data acquisition and analysis were performed using the iCycler real-time PCR detection system (Bio-Rad). All FIV_{pco} reactions were evaluated by melt-curve analysis to confirm the size of the amplicon and lack of primer-dimer formation. Genomic DNA from uninfected cougars did not amplify with FIV_{pco}-specific oligonucleotides.

Reverse transcription (RT) was carried out as a two-step procedure for both the RNA standards and plasma samples. The reaction mixture, 30 µl total, contained 1 µl SuperScript III Reverse Transcriptase (Invitrogen), 4 µl 5 × RT buffer, 1 nM ETaqR and 10 µl purified RNA. The reaction was conducted at 50 °C for 50 min and 85 °C for 5 min.

Plasma viral RNA quantification was determined using 50 µl reactions consisting of 25 µl 2 × Platinum SYBR Green qPCR SuperMix (Invitrogen), 300 nM ETaqF and 300 nM ETaqR. FIV_{pco} amplification was as follows: 50 °C for 2 min followed by 1 cycle of 95 °C for 2 min then a two-step PCR procedure consisting of 95 °C for 15 s then 60 °C for 45 s for 45 cycles.

All standards, negative controls and samples were run in duplicate and the mean value of the copy number was used to quantify both FIV_{pco} and myosin. The measurements of myosin and FIV_{pco}-copy numbers were accepted if the coefficients of variation (CV) were $<20\,\%$ for myosin reactions and $<35\,\%$ for FIV_{pco} reactions. FIV_{pco}-copy number for provirus was divided by the number of cells assayed and reported on the basis of 10^6 PBMC or LN cells. FIV_{pco}-copy number for plasma virus was divided by the volume of plasma assayed and reported as the number of viral RNA copies per millilitre of plasma.

Statistical analysis. The lower limits of detection for the proviral and plasma viral load real-time PCR assays were set at 100 DNA copies and 320 RNA copies per reaction to account for increased variability in cycle number in quantifying low-copy numbers (see Results). Samples that amplified below the lower limit of detection were confirmed by melt-curve analysis.

Proviral and plasma viral loads were determined from PBMC and plasma that were above the lower limit of detection. The mean and standard deviation of both proviral and plasma viral loads were calculated and 95 % confidence intervals were then set for both population means through the Student's *t* distribution. The lower limit of both proviral and plasma viral loads was calculated. The minimum number of cell equivalents and minimum volume of plasma per reaction, which would generate viral loads within the 95 % confidence intervals, were determined to be $1{\cdot}16 \times 10^4$ cells and 100 µl plasma per reaction. Samples assayed that exceeded the calculated minimum of cell equivalents or plasma volume, but had viral loads below the lower limit of real-time detection, were down weighted with a factor of $1/\sqrt{10}$ to account for increased variability in threshold-cycle numbers at low-copy number. Proviral and plasma samples assayed below the calculated minimum of cell equivalents or plasma volume and samples that did not reach threshold were excluded from the statistical analysis.

A weighted univariate analysis of covariance (ANCOVA) was used to test if any significant differences existed among the $\log_{10}$ proviral and plasma viral load means due to differences in age, gender and viral lineage. Levene's test of equality of error variance was used to ensure equal variance existed across the lineages. The proviral model was created based on the ANCOVA of proviral load on age, which resulted in separate slopes and intercepts for each lineage.

RESULTS

Experimental conditions of the FIV_{pco} proviral and plasma viral load real-time PCR assays

A fragment of exon 19 of the cougar myosin gene was used to determine the number of cell equivalents in samples to be quantified for FIV_{pco} provirus. Amplification of the myosin gene producing a standard curve was based on Taqman chemistry and was linear over seven orders of magnitude. The efficiencies (defined as $10^{-1/\text{slope}}$) of the plasmid and genomic samples were 1·90 and 1·91, respectively, indicating that plasmid and genomic DNA amplified with equivalent efficiency in our assay (data not shown). The number of cell equivalents determined for proviral quantifications was established by calculating the mean of two separate myosin quantifications of genomic cougar DNA. The inter-assay variation for myosin quantification was determined by comparing the values obtained for standard curves produced in four separate experiments. Five standards with the low-copy number ($9{\cdot}25 \times 10^4$–$9{\cdot}25 \times 10^0$ copies per reaction) were used in calculating the CV to measure the variation in the most dilute standards (data not shown). The mean threshold cycle (Ct) CV was 1·04 % and the mean absolute CV was 14·52 %. These results demonstrate that the assay used to enumerate cell equivalents is highly reproducible.

Previous work established that mismatches within the real-time primer sites do not enable accurate quantification because of variable efficiencies in amplification (Klein *et al.*, 1999). Because the viral sequence diversity observed among cougar lentiviurses is greater than the diversity observed in FIV in domestic cats (Carpenter *et al.*, 1996), we first established the phylogenetic affiliation of all FIV_{pco} samples prior to quantification and then determined the effect of nucleotide mismatches on FIV_{pco} real-time amplification. All samples clustered within five distinct viral lineages based on a fragment of *env* (Fig. 1). Viral lineage associations were consistent with those in ML trees of *env* and *pol* sequences from 150 individual cougars (Biek *et al.*, 2006). The associations of lineage one and two were consistent with previously published results (Biek *et al.*, 2003).

We prepared separate FIV_{pco} standards from sequences that represented each viral lineage and investigated the effects of these mismatches on amplification efficiency. Lineage standards containing no mismatches or mismatches in one or both primers were evaluated simultaneously by real-time PCR. Standards from three lineages produced overlapping curves and were not significantly different based on an F test for significant differences between lines ($P = 0{\cdot}114$). Although the variation between DNA plasmid standard curves were not significantly different, the error associated with the low-copy number standards increased with the

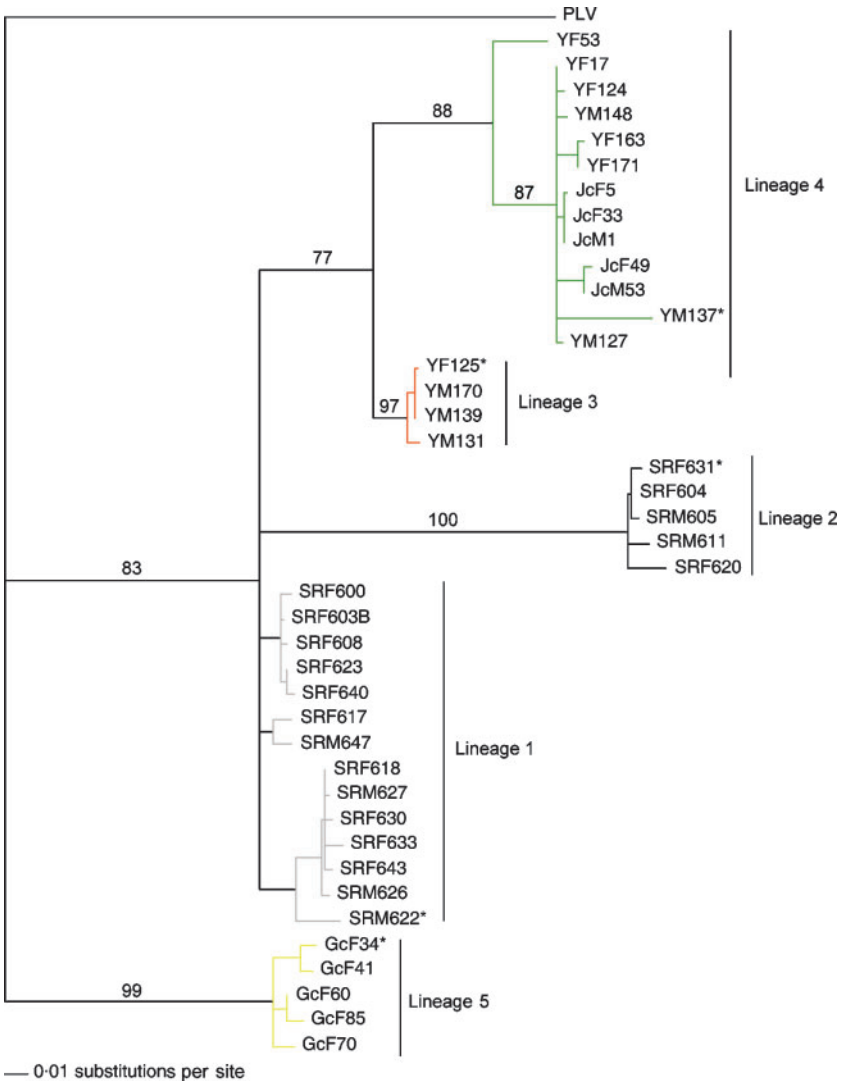

Fig. 1. Phylogenetic relatedness of FIV_{pco} based on *env* sequences. Maximum-likelihood was used to obtain an estimate of the phylogenetic relationship of partial FIV_{pco} *env* sequences from naturally infected cougars. Values at tree nodes represent bootstrap values of $\geqslant 70$ based on 100 bootstrap iterations. PLV was used as an outgroup. The population affiliation and sex for each cougar is indicated before the animal identification number (Y, Yellowstone National Park, MT; SR, Snowy Mountain Range, WY; Gc, Garnet Mountain Range, MT; Jc, Jackson Mountain Range, WY; M, male; and F, female). Sequences used in real-time proviral quantification as plasmid DNA standards are indicated by an asterisk (*).

number of primer mismatches. Therefore, for proviral DNA quantification, a lineage-specific standard was used for samples of each lineage. The mean Ct CV (3·62 %) and the mean absolute CV (38·52 %) was calculated to determine FIV_{pco} inter-assay variation (data not shown). The inter-assay variation of the FIV_{pco} real-time assay was greater than the difference between different FIV_{pco}-lineage standards. The mean absolute FIV_{pco} inter-assay variation, obtained with SYBR green, of 38·52 % is comparable to the variation described previously in real-time assays using Taqman probes, which has been reported to be greater than 35 % (Damond *et al.*, 2001; Desire *et al.*, 2001). CV increased at the low-copy numbers, where the final standard, $6{\cdot}45 \times 10^1$ copies, had the largest CV value (68·33 %). Subsequently, we set the lower limit of detection at 100 DNA copies per reaction to account for the variability associated with the most dilute standard.

For plasma viral load quantification, a two-step real-time PCR assay was developed that was linear over six orders of magnitude from $3{\cdot}2 \times 10^8$ to $3{\cdot}2 \times 10^2$ copies. The lower limit of detection for this assay was set at 320 RNA copies per reaction to account for increased variation in threshold-cycle number with low-copy number standards. Only one RNA standard was amplified in the real-time RT assay because there were no significant differences between separate proviral standards in amplification and virus representative of all five lineages have not been isolated. The inter-assay variation for real-time RT-PCR was 3·92 % for the mean Ct CV and 38·38 % for the mean absolute CV (data not shown). This is similar to the inter-assay variation for the proviral quantification, suggesting that the RT step had minimal effects on assay reproducibility and is also comparable to variation reported for other real-time RT assays (Gibellini *et al.*, 2004; Gueye *et al.*, 2004).

Proviral loads in naturally infected cougars

Cougar samples quantified in this study were determined previously to be FIV_{pco}-positive by nested PCR. Therefore,

the FIV_{pco} real-time PCR assay was utilized only to quantify viral loads and was not used as a detection method. Thirty-nine cougar PBMC samples were quantified and 22 (56 %) were within our level of detection (Table 1). Ten LN samples were also quantified and five were within the range of detection (50 %). Samples that had less than 100 proviral copies, which we established as the lower limit of detection, were still valuable in our analysis. For example, FIV_{pco}-copy number was below the limit of detection in four PBMC and two LN samples despite the fact that more than 1×10^5 cell

Table 1. Age and gender data of infected cougars and lineage affiliation of FIV_{pco} and amount of provirus and plasma virus detected from each animal using real-time PCR

Lineage	Cat ID no.	Age (years)	Proviral load per 10^6 PBMC	Plasma viral load ml^{-1}
1	SRF640	0·4	ND	519 000
	SRF603B	0·5	4 087	ND
	SRM647	0·8	472*	ND
	SRF630	1·3	4 746	50 243
	SRF633	1·6	8 805	ND
	SRF608	2·0	4 567	10 529*
	SRF643	2·5	ND	678 857
	SRF600	3·0	1 848	ND
	SRM622	3·5	9 712	ND
	SRM626	3·5	3 447	ND
	SRM627	3·5	17 788	ND
	SRM626	4·5	ND	29 880
	SRF618	5·5	46 575	ND
	SRF623	5·5	21 721	ND
	SRF617	8·5	ND	74 880
2	SRF620	1·8	879*	ND
	SRF620	2·8	ND	169 059
	SRM605	4·5	30 095	ND
	SRF604	5·5	18 885	ND
	SRM611	5·5	4 982	ND
3	YF171	0·5	67 188	925 200
	YM170	2·0	ND	542 466
	YM139	4·5	ND	5 292*
	YM131	5·7	ND	302 400
	YF125	7·5	2 913	183 000
	YM148	9·5	1 826	768 000
4	JcF06	2·8	ND	804 600
	JcM49	4·0	41 940	ND
	YF124	4·6	ND	14 508
	YM127	5·7	4 589	2 295*
	YM163	6·5	29*	2 805 000
	JcF33	6·5	10 014	ND
	JcM01	8·0	220*	205 527
	YM137	8·3	ND	8 344
	JcF05	10·0	2 681*	54 000
	YF53	11·0	4 943	28 337
	YF17	13·0	386*	ND
5	GcF85	0·9	41 485	ND
	GcF41	1·2	17 534	ND
	GcF41	2·4	ND	42 742
	GcF70	4·0	1 818*	ND
	GcF60	4·5	ND	84 185
	GcF34	6·4	336*	146 700

*Indicates down weighted proviral or plasma viral loads.
ND, Not determined.

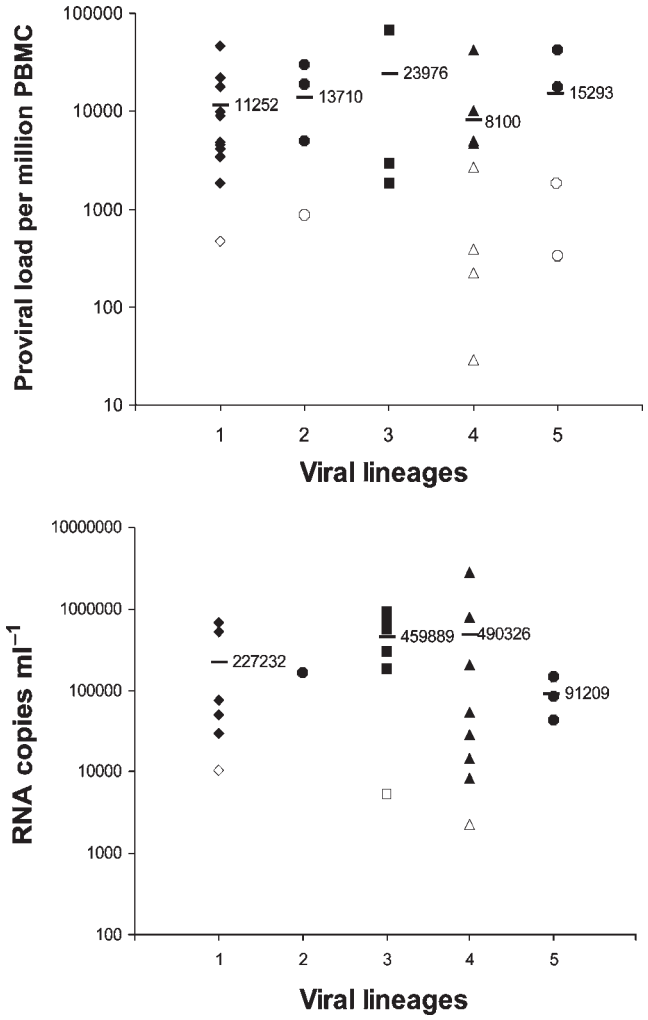

Fig. 2. FIV_{pco} proviral and plasma viral load for each viral lineage. The mean values for each viral lineage are shown next to the horizontal lines. Closed shapes denote proviral or plasma viral loads that were within the detection limits established for this assay. Open shapes denote down weighted proviral or plasma viral loads.

equivalents were assayed, indicating that the proviral load was low in those animals. Therefore, 95 % confidence intervals for the number of cells required for FIV_{pco} detection was established (see Methods). Samples that were adequately assayed but below detection were down weighted to account for increased variability associated with threshold-cycle number. Eight PBMC samples were down weighted in the proviral analysis. Samples for which there were insufficient cell numbers or plasma volume for adequate sampling were omitted from the statistical analysis. Nine PBMC samples were omitted from the proviral analysis.

The mean proviral load per 10^6 PBMC was $1{\cdot}34 \times 10^4$ and ranged from $2{\cdot}9 \times 10^1$ to $6{\cdot}72 \times 10^4$ (Fig. 2). The lowest proviral loads were adequately assayed, however, the number of proviral copies quantified was below our limit of detection. Therefore, these samples were down weighted. The mean proviral load per 10^6 LN cells was $1{\cdot}51 \times 10^4$ (range from $8{\cdot}06 \times 10^3$ to $2{\cdot}51 \times 10^4$). These data indicate that a mean of 1 in 75 circulating cells is infected with FIV_{pco} and 1 in 66 cells in the LN is infected, assuming one proviral FIV_{pco} molecule per cell.

We tested the hypothesis that mean proviral loads in PBMC were equal among gender, age and viral lineage using a weighted ANCOVA. These factors were considered because one or all may have a significant biological effect on the amount of virus in infected cougars. For example, the amount of virus in FIV-infected domestic cats differs significantly between different field isolates (Pedersen *et al.*, 2001). The variation in proviral load was determined to be equal across viral lineages through Levene's test of equality of error variance ($P=0{\cdot}239$). Proviral loads were significantly different between lineages ($P=0{\cdot}029$) and there was a significant interaction between viral lineage and cougar age, indicating that considered together these variables had an effect on proviral load ($P=0{\cdot}014$). No correlation was observed between proviral load and gender ($P=0{\cdot}440$).

Univariate analysis of covariance demonstrates whether differences between means are statistically significant but not how means differ. Therefore, to understand the influence of age and lineage on proviral loads, the linear regression from the ANCOVA of proviral load on age was conducted to model the change in lineage-specific proviral loads versus age, which resulted in separate lines for each lineage (r^2 value $=0{\cdot}549$) (Fig. 3). Cougars infected with viruses from either lineage one or two have an increase in

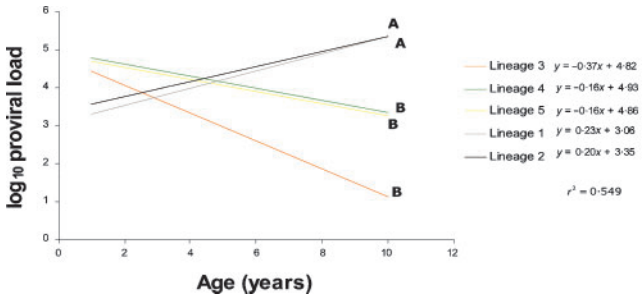

Fig. 3. A weighted analysis of covariance of cougar PBMC proviral loads versus cougar age. The colours for each viral lineage correspond to the phylogeny displayed in Fig. 1. The change in lineage-specific proviral loads versus cougar age was based on an ANCOVA of cougar PBMC proviral loads with viral lineage and gender as factors and age as a covariate. Lineage-specific PBMC proviral loads were averaged across gender because gender was not a significant influence on PBMC proviral loads. The linear regressions of proviral loads from lineages one and two, indicated with A, were statistically different from those of lineages three, four and five, indicated with B ($P \leqslant 0{\cdot}05$). However, the differences observed between lineages three, four and five were not significant ($P > 0{\cdot}24$).

PBMC proviral loads with age. In contrast, cougars infected with viruses from either lineage three, four or five exhibit a decrease in proviral loads with age. The differences between lineages three, four and five or between lineage one and two were not significant ($P>0{\cdot}24$). However, the linear regression of proviral loads from lineages one and two were statistically different from those of lineages three, four and five ($P\leqslant 0{\cdot}05$) and this difference remained after random deletion of three proviral load values.

Plasma viral load in naturally infected cougars

Thirty-two plasma samples were quantified and in 21 (66 %) of these samples FIV_{pco} was detectable by our real-time assay (Table 1). The plasma viral loads ranged from $2{\cdot}30\times10^3$ to $2{\cdot}81\times10^6$ RNA copies ml^{-1}, with a mean of $5{\cdot}69\times10^5$ (Fig. 2). Of the 11 plasma samples that were below our limit of detection, eight samples were not included in the statistical analysis because an insufficient volume of plasma was assayed and three samples were down weighted as described previously. The variance in plasma viral loads was determined to be equal across lineages through Levene's test ($P=0{\cdot}086$). Through a univariate ANCOVA no significant differences were observed between mean plasma viral loads for different genders, ages or lineages ($P=0{\cdot}958$, $0{\cdot}830$ and $0{\cdot}783$, respectively). Additionally, we were able to quantify proviral and plasma viral loads from the same blood sample of 11 cougars in the study (Fig. 4). There was no correlation between proviral and plasma viral loads (r^2 value $=0{\cdot}133$) from the same individual. Similarly, there was no correlation between FIV_{pco} plasma viral loads and PBMC proviral loads within viral lineages (data not shown). These data demonstrate that the level of plasma viraemia is not correlated to the number of infected PBMC, age, gender or viral lineage.

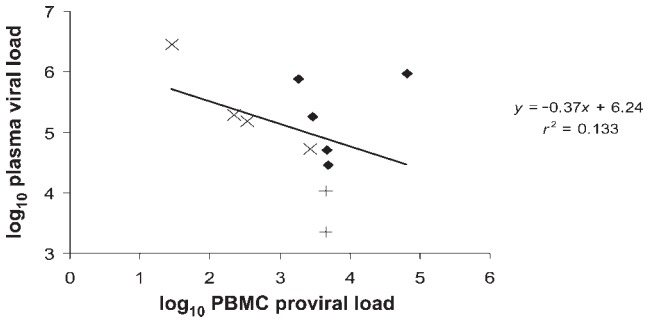

Fig. 4. Correlation of PBMC proviral loads versus plasma viral loads of infected cougars. Proviral and plasma viral loads were quantified from the same blood sample of 11 cougars. All samples had at least one viral load parameter that was within the detection threshold. Diamonds denote proviral and plasma viral loads within the detection threshold. Down weighted proviral loads are indicated with '×' and '+' denotes down weighted plasma viral loads.

DISCUSSION

Free-ranging cougars are one of several feline species that harbour an endemic lentivirus infection without any apparent signs of disease (Biek *et al.*, 2005; Brown *et al.*, 1994; Carpenter & O'Brien, 1995; Olmsted *et al.*, 1992; Packer *et al.*, 1999). However, it was not known if the lack of disease observed in naturally infected cougars was a result of low-level virus replication. Consequently, FIV_{pco} proviral and plasma viral loads were quantified from naturally infected cougars by real-time PCR. This study represents the most extensive analysis of proviral and plasma viral loads in natural, endemic lentivirus infections to date.

Proviral loads reported previously in infected PBMC from African green monkeys and sooty mangabeys are in the order of 10^2–10^3 proviral copies per 10^6 cells, respectively (Beer *et al.*, 1996; Broussard *et al.*, 2001; Rey-Cuille *et al.*, 1998). The mean cougar PBMC proviral load was $1{\cdot}34\times10^4$ proviral copies per 10^6 cells. Therefore, FIV_{pco} proviral loads in infected PBMC are in order of magnitude higher than in PBMC from infected primates. The mean LN proviral load, which was determined from a separate group of infected cougars, was $1{\cdot}51\times10^4$ proviral copies per 10^6 cells. Although the variation around LN proviral loads was markedly lower than in PBMC, both cougar PBMC and LN cells had similar mean proviral loads. Equivalent PBMC and LN proviral loads have been reported previously in a large cohort of long-term naturally infected African green monkeys (Beer *et al.*, 1996). These data stand in contrast to other studies that have reported elevated proviral loads in lymphoid tissue in naturally infected primates and HIV-1-infected humans (Broussard *et al.*, 2001; Fauci *et al.*, 1996). Finally, plasma viral loads in naturally infected cougars ranged from 10^3 to 10^6 RNA copies ml^{-1} and are comparable to viraemia levels reported previously in SIV_{sm} and SIV_{agm} infections (Broussard *et al.*, 2001; Goldstein *et al.*, 2000; Holzammer *et al.*, 2001; Rey-Cuille *et al.*, 1998). These data clearly indicate that the absence of detectable disease in naturally infected cougars and primates is not a result of low-level virus replication.

In pathogenic lentivirus infections, such as HIV-1 or FIV in domestic cats, the amount of circulating virus is an accurate predictor of disease severity. In humans and domestic cats, plasma viral loads greater than 10^5 copies ml^{-1} are correlated to disease progression and shorter survival time (Goto *et al.*, 2002; Mellors *et al.*, 1996). FIV_{pco}-infected cougars maintain plasma viral loads that are greater than 10^5 copies ml^{-1} during infection, but these animals remain asymptomatic. Furthermore, we could not detect any relationship between plasma viral loads in infected cougars and factors such as age, gender or viral lineage. Different rates of cell-free virus clearance and production have been reported in patients infected with HIV-1, but the lifespan of infected cells was not significantly different among patients (Perelson *et al.*, 1996). The lack of correlation in plasma viral loads with age, gender or virus lineage may reflect the

transient nature of cell-free virus compared with the integrated provirus.

There was no correlation between the FIV_{pco} and PBMC proviral loads in 11 infected cougars from which both plasma and blood were available. In fact, the animal with the highest plasma viral load ($2{\cdot}81 \times 10^6$) maintained a proviral load that was below the lower limit of detection (Fig. 4). These data suggest that circulating PBMC may not be the primary source of FIV_{pco} particles in the blood. This is consistent with studies of HIV-1 infection, which established that the primary site of virus production is lymphoid tissue (Haase, 1999) and greater than 90 % of HIV-1 plasma viraemia is maintained by a fraction of the $CD4^+$ T-cell population (Hufert *et al.*, 1997).

The widespread distribution of FIV_{pco} in North America and the extensive sequence divergence between FIV_{pco} lineages indicate that FIV_{pco} infection in free-ranging cougars is not a recent event (Carpenter *et al.*, 1996). In addition, the lack of disease may be an outcome of coevolution between FIV_{pco} and its cougar host (Carpenter & O'Brien, 1995). Based on our data, the low FIV_{pco} intrahost viral diversity reported previously (Biek *et al.*, 2003) cannot be attributed to low-level virus replication and may be a result of other factors including an absence of strong-positive selection on the virus, an increased fidelity of the FIV_{pco} reverse transcriptase or longer virus generation time. Additionally, the high cell-associated and cell-free viral loads documented in infected cougars perhaps may be an effective mechanism by which FIV_{pco} can sustain a high prevalence rate (30–58 %) in a solitary species (Biek *et al.*, 2003; Carpenter *et al.*, 1996). Indeed, both FIV cell-associated and cell-free virus are able to cause infection in domestic cats (Burkhard *et al.*, 1997).

Our results indicate that over half of the variability in PBMC proviral loads can be ascribed to viral lineage and cougar age (r^2 value $= 0{\cdot}549$). Although the number of PBMC samples quantified was moderate ($n = 30$), there was a strong correlation of PBMC proviral loads to viral lineage and cougar age ($P = 0{\cdot}014$). Because differences in proviral loads among viral lineages were most pronounced in adult cougars (Fig. 3), changes in hormone levels associated with sexual maturation or activity may influence virus replication. Activation of viral transcription occurs in type B (mouse mammary tumour virus) and type C (murine leukaemia virus) retroviruses in response to adrenal steroids by binding their respective receptors to hormone response elements located within the long terminal repeat (Cato *et al.*, 1988; Miksicek *et al.*, 1986). Therefore, the physiological state of a maturing infected cougar may influence virus replication and ultimately affect the number of infected circulating cells. Such a replication strategy could optimize viral transmission during contact events. Interestingly, animals infected with viruses from lineage one and two, which displayed an increase in proviral load with age, are from the population with the highest prevalence of FIV_{pco} infection (Biek *et al.*, 2003), suggesting that this strategy leads to a higher likelihood of transmission.

In summary, quantification of FIV_{pco} proviral and plasma viral loads has established that infected cougars maintain substantial viral loads that are comparable or higher than those reported in endemic primate lentivirus infections. These data further support the premise that high levels of lentivirus replication do not necessarily correlate with disease. Finally, differences observed in cougar PBMC proviral loads correlated to viral lineage and host age, suggesting that different life strategies exist within FIV_{pco} lineages.

ACKNOWLEDGEMENTS

This work was partially funded by grants from the Morris Animal Foundation DO1Z0-111, the NIH AI54303 and AI52055, and NIH Grant no. P20 RR16455-03 from the INBRE-BRIN Program of the National Center for Research Resources. The authors thank W. Holben for use of the iCycler thermal cycler, R. Biek and E. Burkala for critical reading of the manuscript, and K. Ferris and S. Painter for technical assistance.

REFERENCES

Beer, B., Scherer, J., zur Megede, J., Norley, S., Baier, M. & Kurth, R. (1996). Lack of dichotomy between virus load of peripheral blood and lymph nodes during long-term simian immunodeficiency virus infection of African green monkeys. *Virology* **219**, 367–375.

Biek, R., Rodrigo, A. G., Holley, D., Drummond, A., Anderson, C. R., Jr, Ross, H. A. & Poss, M. (2003). Epidemiology, genetic diversity, and evolution of endemic feline immunodeficiency virus in a population of wild cougars. *J Virol* **77**, 9578–9589.

Biek, R., Ruth, T. K., Murphy, K. M., Anderson, C. R. & Poss, M. (2005). Examining effects of persistent retrovirus infection on fitness and pathogen susceptibility in a natural feline host. *Can J Zoo* (in press).

Biek, R., Drummond, A. & Poss, M. (2006). A virus reveals population structure and recent demographic history of its carnivore host. *Science* **311**, 538–541.

Broussard, S. R., Staprans, S. I., White, R., Whitehead, E. M., Feinberg, M. B. & Allan, J. S. (2001). Simian immunodeficiency virus replicates to high levels in naturally infected African green monkeys without inducing immunologic or neurologic disease. *J Virol* **75**, 2262–2275.

Brown, E. W., Yuhki, N., Packer, C. & O'Brien, S. J. (1994). A lion lentivirus related to feline immunodeficiency virus: epidemiologic and phylogenetic aspects. *J Virol* **68**, 5953–5968.

Burkhard, M. J. & Dean, G. A. (2003). Transmission and immunopathogenesis of FIV in cats as a model for HIV. *Curr HIV Res* **1**, 15–29.

Burkhard, M. J., Obert, L. A., O'Neil, L. L., Diehl, L. J. & Hoover, E. A. (1997). Mucosal transmission of cell-associated and cell-free feline immunodeficiency virus. *AIDS Res Hum Retroviruses* **13**, 347–355.

Carpenter, M. A. & O'Brien, S. J. (1995). Coadaptation and immunodeficiency virus: lessons from the Felidae. *Curr Opin Genet Dev* **5**, 739–745.

Carpenter, M. A., Brown, E. W., Culver, M., Johnson, W. E., Pecon-Slattery, J., Brousset, D. & O'Brien, S. J. (1996). Genetic and

phylogenetic divergence of feline immunodeficiency virus in the puma (*Puma concolor*). *J Virol* **70**, 6682–6693.

Cato, A. C., Skroch, P., Weinmann, J., Butkeraitis, P. & Ponta, H. (1988). DNA sequences outside the receptor-binding sites differently modulate the responsiveness of the mouse mammary tumour virus promoter to various steroid hormones. *EMBO J* **7**, 1403–1410.

Chakrabarti, L. A. (2004). The paradox of simian immunodeficiency virus infection in sooty mangabeys: active viral replication without disease progression. *Front Biosci* **9**, 521–539.

Damond, F., Descamps, D., Farfara, I. & 7 other authors (2001). Quantification of proviral load of human immunodeficiency virus type 2 subtypes A and B using real-time PCR. *J Clin Microbiol* **39**, 4264–4268.

Desire, N., Dehee, A., Schneider, V., Jacomet, C., Goujon, C., Girard, P. M., Rozenbaum, W. & Nicolas, J. C. (2001). Quantification of human immunodeficiency virus type 1 proviral load by a TaqMan real-time PCR assay. *J Clin Microbiol* **39**, 1303–1310.

Diehl, L. J., Mathiason-Dubard, C. K., O'Neil, L. L. & Hoover, E. A. (1996). Plasma viral RNA load predicts disease progression in accelerated feline immunodeficiency virus infection. *J Virol* **70**, 2503–2507.

Fauci, A. S., Pantaleo, G., Stanley, S. & Weissman, D. (1996). Immunopathogenic mechanisms of HIV infection. *Ann Intern Med* **124**, 654–663.

Gibellini, D., Vitone, F., Schiavone, P., Ponti, C., La Placa, M. & Re, M. C. (2004). Quantitative detection of human immunodeficiency virus type 1 (HIV-1) proviral DNA in peripheral blood mononuclear cells by SYBR green real-time PCR technique. *J Clin Virol* **29**, 282–289.

Goldstein, S., Ourmanov, I., Brown, C. R., Beer, B. E., Elkins, W. R., Plishka, R., Buckler-White, A. & Hirsch, V. M. (2000). Wide range of viral load in healthy African green monkeys naturally infected with simian immunodeficiency virus. *J Virol* **74**, 11744–11753.

Goto, Y., Nishimura, Y., Baba, K., Mizuno, T., Endo, Y., Masuda, K., Ohno, K. & Tsujimoto, H. (2002). Association of plasma viral RNA load with prognosis in cats naturally infected with feline immunodeficiency virus. *J Virol* **76**, 10079–10083.

Gueye, A., Diop, O. M., Ploquin, M. J., Kornfeld, C., Faye, A., Cumont, M. C., Hurtrel, B., Barre-Sinoussi, F. & Muller-Trutwin, M. C. (2004). Viral load in tissues during the early and chronic phase of non-pathogenic SIVagm infection. *J Med Primatol* **33**, 83–97.

Haase, A. T. (1999). Population biology of HIV-1 infection: viral and $CD4^+$ T cell demographics and dynamics in lymphatic tissues. *Annu Rev Immunol* **17**, 625–656.

Holzammer, S., Holznagel, E., Kaul, A., Kurth, R. & Norley, S. (2001). High virus loads in naturally and experimentally SIVagm-infected African green monkeys. *Virology* **283**, 324–331.

Hufert, F. T., van Lunzen, J., Janossy, G., Bertram, S., Schmitz, J., Haller, O., Racz, P. & von Laer, D. (1997). Germinal centre $CD4^+$ T cells are an important site of HIV replication in vivo. *AIDS* **11**, 849–857.

Klein, D., Janda, P., Steinborn, R., Muller, M., Salmons, B. & Gunzburg, W. H. (1999). Proviral load determination of different feline immunodeficiency virus isolates using real-time polymerase chain reaction: influence of mismatches on quantification. *Electrophoresis* **20**, 291–299.

Mellors, J. W., Rinaldo, C. R., Jr, Gupta, P., White, R. M., Todd, J. A. & Kingsley, L. A. (1996). Prognosis in HIV-1 infection predicted by the quantity of virus in plasma. *Science* **272**, 1167–1170.

Miksicek, R., Heber, A., Schmid, W., Danesch, U., Posseckert, G., Beato, M. & Schutz, G. (1986). Glucocorticoid responsiveness of the transcriptional enhancer of Moloney murine sarcoma virus. *Cell* **46**, 283–290.

Muller-Trutwin, M. C., Corbet, S., Tavares, M. D., Herve, V. M., Nerrienet, E., Georges-Courbot, M. C., Saurin, W., Sonigo, P. & Barre-Sinoussi, F. (1996). The evolutionary rate of nonpathogenic simian immunodeficiency virus (SIVagm) is in agreement with a rapid and continuous replication in vivo. *Virology* **223**, 89–102.

Olmsted, R. A., Langley, R., Roelke, M. E. & 12 other authors (1992). Worldwide prevalence of lentivirus infection in wild feline species: epidemiologic and phylogenetic aspects. *J Virol* **66**, 6008–6018.

Packer, C., Altizer, S., Appel, M., Brown, E., Martenson, J., O'Brien, S. J., Roelke-Parker, M., Hofmann-Lehmann, R. & Lutz, H. (1999). Viruses of the Serengeti: patterns of infection and mortality in African lions. *J Anim Ecol* **68**, 1161–1178.

Pedersen, N. C., Ho, E. W., Brown, M. L. & Yamamoto, J. K. (1987). Isolation of a T-lymphotropic virus from domestic cats with an immunodeficiency-like syndrome. *Science* **235**, 790–793.

Pedersen, N. C., Leutenegger, C. M., Woo, J. & Higgins, J. (2001). Virulence differences between two field isolates of feline immunodeficiency virus (FIV-$A_P$etaluma and FIV-C_{PG}ammar) in young adult specific pathogen free cats. *Vet Immunol Immunopathol* **79**, 53–67.

Perelson, A. S., Neumann, A. U., Markowitz, M., Leonard, J. M. & Ho, D. D. (1996). HIV-1 dynamics in vivo: virion clearance rate, infected cell life-span, and viral generation time. *Science* **271**, 1582–1586.

Posada, D. & Crandall, K. A. (1998). MODELTEST: testing the model of DNA substitution. *Bioinformatics* **14**, 817–818.

Rey-Cuille, M. A., Berthier, J. L., Bomsel-Demontoy, M. C., Chaduc, Y., Montagnier, L., Hovanessian, A. G. & Chakrabarti, L. A. (1998). Simian immunodeficiency virus replicates to high levels in sooty mangabeys without inducing disease. *J Virol* **72**, 3872–3886.

Shankarappa, R., Margolick, J. B., Gange, S. J. & 9 other authors (1999). Consistent viral evolutionary changes associated with the progression of human immunodeficiency virus type 1 infection. *J Virol* **73**, 10489–10502.

Swofford, D. L. (2002). PAUP* Phylogenetic Analysis Using Parsimony (*and Other Methods). Version 4.0b10 Sunderland, MA: Sinauer Associates.